Intracellular pharmacodynamic modelling (*PDi*) is predictive of the clinical activity of fluoroquinolones against Tuberculosis

Samantha Donnellan[a†], Ghaith Aljayyoussi[a†], Emmanuel Moyo[a], Alison Ardrey[a], Carmen Martinez-Rodriguez[b], Stephen A Ward[a] and Giancarlo A Biagini[a*]

[†] These authors contributed equally to this manuscript

* For correspondence please email: giancarlo.biagini@lstmed.ac.uk +44 (0)151 705 3151 Fax: +44(0)151 705 3370

a. Centre for Drugs and Diagnostics, Department of Tropical Disease Biology, Liverpool School of Tropical Medicine, Pembroke Place, Liverpool, L3 5QA, United Kingdom.

b. Institute of Infection and Global Health, University of Liverpool, 8 West Derby Street, Liverpool, L69 7BE, United Kingdom.

Abstract

Clinical studies of new anti-tubercular drugs are costly and time consuming. Owing to the extensive TB treatment periods, the ability to identify drug candidates based on their predicted clinical efficacy is vital to accelerate the pipeline of new therapies. Recent failures of pre-clinical models in predicting the activity of fluoroquinolones underlines the importance of developing new and more robust predictive tools that will optimise the design of future trials. Here, we have used high-content imaging screening and pharmacodynamic intracellular modelling (*PDi*) to identify and prioritise fluoroquinolones for TB treatment. In a set of studies designed to validate this approach, we show moxifloxacin to be the most effective fluoroquinolone, and *PDi* modelling-based Monte Carlo simulations accurately predict negative culture conversion (sputum sterilisation) rates when compared against 8-independent clinical trials. Additionally, *PDi*-based simulations were used to predict the risk of relapse. Our analyses show that the duration of treatment following culture conversion can be used to predict relapse rate. These data further support that *PDi*-based modelling offers a much-needed decision making tool for the TB drug development pipeline.

Introduction

Tuberculosis (TB) caused by *Mycobacterium tuberculosis* (*Mtb*), is the leading cause of death from a single infectious agent. The so-called short course treatment of drug-susceptible TB (2-month intensive phase of Rifampicin [RIF], Isoniazid [INH], Pyrazinamide [PZA] and Ethambutol [EMB] then 4-months of RIF and INH) (1) remains long, complex and expensive, with relatively high results of failure due to patient non-compliance and drug resistance. Fluoroquinolones, were introduced into the regimen for multi-drug resistant TB (MDR-TB) after demonstration of their *in vitro* and *in vivo* anti-mycobacterial activity (2–6). They are now considered by the WHO to be a critical component in MDR-TB treatment. Fluoroquinolones are also administered when patients cannot tolerate the standard regimen (7). However, fluoroquinolones, especially third generation, are often discussed in terms of a generic

drug class and the specific choice of fluoroquinolone is generally not specified and is therefore often based on availability, cost and national guidelines.

It was anticipated that by introducing fluoroquinolones into drug-susceptible regimens, the treatment period could be reduced by 2-months (from 6 to 4) (8). Clinical trials with moxifloxacin (MXF) produced mixed results, with some displaying superior activity that would indicate shorter treatment courses (9, 10) but others displaying little, to no acceleration in achieving negative culture conversion (11, 12). However, a recent meta-analysis of all clinical data showed a significant improvement of culture conversion rates in total (13).

Pharmacokinetic/Pharmacodynamic (PK/PD) models are useful in evaluating the length of treatment required by new regimens of anti-TB drugs. Recent clinical trials have highlighted the concerns of preclinical studies. Animal models show dynamics that differ to those observed in humans (14, 15) and predicted treatment improvements observed in mice with reformed regimens have often failed to reflect similar results in clinical settings. For example, murine studies with rifamycins (16–18) over-predicted the superior activity of higher doses of rifapentine in clinical studies. Similarly, animal studies were interpreted as showing a significant potential for the reduction in time of TB treatment with MXF, (19) suggesting that treatment could be reduced by 1-month based on the *in vivo* results (20). However, phase 3 clinical trials (e.g. REMOX and RIFAQUIN) highlighted that despite the superiority of MXF, it was insufficient to display relapse-free cure rates observed in 6-months of conventional TB therapy (11, 21).

We have previously shown that PD data obtained from an *in vitro* intracellular (macrophage) *Mtb* high-content imaging-based platform, termed intracellular pharmacodynamics (*PDi*), can be a powerful tool for predicting the activity of first line TB drugs in patients (22). Our platform is capable of defining the killing kinetics of first line anti-TB drugs against intracellular *Mtb.* Building from this previous work, and using a refined method that allows for extended monitoring of live drug-exposed intracellular *Mtb*, here we profile fluoroquinolones to assess their anti-tubercular efficacy. In addition, using this data we have performed *PDi* -based

PK/PD predictions of clinical outcome in terms of culture conversion rates and compare these values with clinical studies. Data is discussed in the context of the use of fluoroquinolones towards shortening treatment duration and the value of the *PDi* - based approach as a decision-making tool in the drug development of new treatment therapies.

Results

Fluoroquinolones exhibit comparable rates of kill against intracellular *Mtb,* but differ in potency

The efficacy of selected fluoroquinoles against intracellular Mtb was initially determined using the described fluorimetric-based assay (see methods). The intracellular anti-tubercular activity of MXF, levofloxacin (LVX), norfloxacin (NOX), ofloxacin (OFX), sparfloxacin (SPX), and ciprofloxacin (CIP) was assessed at a concentration range between 0.01 mg/L – 100 mg/L. The kill rate elicited by each concentration was then calculated as previously described (22). Figure 1 displays the kill rate for each drug's concentration range. A concentration-effect relationship using a three-parameter pharmacological model was then determined for each drug (Fig. 2). This model affords the calculation of pharmacological parameters, namely EC_{50} and maximal kill rates for each drug (Fig. 2 a-f). Figure 2 (g) compares the profiles of all drugs where the grey area represents the kill rate of RIF (first-line antibiotic) at 25 mg/L (chosen as it is 1000 fold the EC_{50} concentration and is used to determine the E_{max}, see Methods).

The fluoroquinolones tested displayed variability in potency for their respective intracellular anti-TB activity. SPX displayed the lowest EC_{50} (0.051 mg/L), followed by MXF, CIP and LVX (0.238 mg/L, 0.259 mg/L and 0.382 mg/L respectively) whilst OFX and NOX displayed poor activity with EC_{50} levels of 1.414 mg/L-1.705 mg/L as shown in Figures 1-2 and Table S1. Of note, although fluoroquinolones displayed variation in EC_{50} values, the maximal kill rate for all fluoroquinolones was determined to be comparable (Fig. 2g) – consistent with the drugs possessing the same mode of action.

Similar to our previous work with RIF, INH and EMB (22) , MXF kill rate of *Mtb* grown in culture, termed extracellular, was significantly faster than the kill rate of MXF against intracellular (macrophage) *Mtb* (0.23 h^{-1} extracellular Vs. 0.055 intracellular, Fig. S1, and Fig. 1, respectfully)

Determination of the *Mtb* growth-kill rate ratio for fluoroquinolones

The above described live *Mtb* fluorimetry-based assay allowed for rapid determination of kill rate EC_{50} for the described fluoroquinolones, using a population-based fluorometric readout of intracellular *Mtb*. To define the maximal killing rate for the fluoroquinolone class at greater resolution and dynamic range, killing dynamics were measured using the Operetta-based high content imaging screen, which can image individual bacilli residing inside macrophages (Fig. 3).

Figure 3 displays intracellular *Mtb* in the absence (a) or presence of MXF (b) (63 x magnification), (c) shows the maximal kill rate displayed by MXF (100 mg/L) compared to RIF at a concentration of 25 mg/L. The maximal kill rate of both drugs was equivalent and measured approximately -1.8 × no drug control growth rate. This concurs with the maximal 'kill: growth' ratio previously reported for RIF (22). Our results demonstrate that despite RIF being the superior compound, by way of a lower EC_{50} value (0.019 mg/L RIF Vs. 0.238 mg/L MXF), the kill rate : growth rate ratio of MXF at a maximal concentration (100 mg/L) was 1.82 – similar to that of RIF at a maximal concentration (Fig. 3 & Fig. S2and Fig. S3).

***PDi* modelling predicts culture conversion rates when compared with clinical trial data**

MXF data from the Operetta based high content imaging screen was modelled and compared to clinical trial data reported in the literature. *PDi* modelling was performed for MXF using PD data obtained from the Operetta study. PK data and pulmonary exposure were calculated for MXF as reported when administered

concomitantly with RIF as all simulations assumed concomitant administration of the two drugs (23, 24). Epithelial lining fluid (ELF) concentrations were used as a surrogate for pulmonary exposure and were obtained from the literature as estimated in healthy volunteers (25, 26). In the absence of such ratios in TB patients, we used healthy volunteer data as the closest possible estimate.

PDi modelling was used to generate COX regression curves. The curves indicate percentage of patients achieving culture-negative conversion over time (culture conversion to negative is defined as <10 CFU/mL in sputum tests) (27).

To compare our predictions with the clinical literature, we used Monte Carlo simulations to generate hypothetical treatment outcomes when using the same regimens previously used in clinical trials. *PDi* modelling predicted that within 8-weeks, 96% of patients would achieve culture-negative status when INH or ETB is replaced with 400 mg MXF (PK/PD properties of partner drugs were based on (22) as shown in Table S1). Our results concur with several clinical studies, as displayed in Table S2 and Figure 4. *PDi* based odds ratios were estimated to be 1.726 (CI: 1.216-2.45) which compares with reported or calculated ratios from clinical literature data (Table S2, Fig. 4). *PDi* prediction of culture conversion rates for MXF containing regimens seems to be marginally faster than that observed in the most comprehensive study (11). However, our prediction is in line with the median of 8 different clinical studies over 8 weeks (Fig. 4b and Table S2).

Table S3 displays the sensitivity analysis of the *PDi* modelling (see Methods), which indicates that the maximal kill rate (E_{max}) of MXF is the most influential parameter upon bacillary clearance. The second most significant parameter is the initial intracellular burden the patient presents at the clinic, concurring with previous clinical studies (28, 29), followed by the PK parameters and MXF drug potency (EC_{50}). Potency and PK parameters of RIF ranked lower than MXF parameters in our sensitivity analysis. Parameters for other partner drugs (INH, EMB or PZA) played a negligible role in the overall outcome of the simulations.

Higher concentrations of LVX is predicted to be as effective as MXF at killing *Mtb*

As the *PDi* model is ultimately based on pulmonary exposure (i.e. concentration in ELF) we compared the overall PK properties and the ELF exposures of MXF, CIP and LVX (Table S4). Simulations predict MXF to have superior PK properties due to its relatively high AUC level in the plasma, and it displays the highest accumulation in the ELF. Table S4 shows that LVX at a higher dose of 750 mg/day would achieve a very similar pulmonary PK profile to that observed for MXF at 400 mg/day. Assuming linear PK for LVX, 500 mg/day is expected to achieve inferior ELF exposure to 400 mg/day of MXF. At 1000 mg dose, LVX has a comparable ELF AUC value (221.7 mg.h/L) compared to a standard dose of MXF of 400 mg/day (173.1 mg.h/L). Systematic PK parameters were chosen from previously reported data as per Table S4.

Simulating various doses of LVX and MXF and integrating this with our imaging-based *PDi* data, reveals that an increase of LVX from 500 mg to 1000 mg results in a remarkable improvement in activity (88% of patients predicted to achieve negative culture conversion at 8 weeks with 500 mg LVX Vs. 93% of patients predicted to achieve negative culture conversion at 8 weeks with 1000 mg LVX, Fig. 5). In contrast, we predict that an increase in the dose of MXF from 400 mg to 800 mg would result in a more modest improvement (95% of patients to achieve culture negative status with 400 mg MXF Vs. 96% with MXF 800 mg) (Fig. 5).

Using *PDi* -based modelling to predict TB treatment duration and risk of relapse

As described, fluoroquinolones have been clinically assessed in efforts to shorten standard therapy (7, 20, 30). We believe culture conversion is related to relapse rates and hypothesise that following culture conversion, further therapy is required to kill hidden/recalcitrant bacilli populations. Figure 6 displays how many patients would hypothetically be at risk of disease relapse when comparing the standard regimen to a MXF arm for 4 or 5-months. We hypothesise that this is directly related to the time taken to culture convert during treatment, which will differ between all patients. As

shown, 6% of patients in the standard treatment arm will culture convert late (<80 days before end of treatment), and therefore not receive treatment for 80 days post conversion, compared to 15% in the 4-month MXF and 4% in the 5-month MXF arm.

Discussion

PDi modelling has previously been utilised for the prediction of treatment outcome for TB patients receiving standard or high dose RIF therapy (22, 31) Herein, we have used a similar approach to predict treatment outcomes using fluoroquinolone-based regimens. Fluoroquinolones have been considered by many to be a means of shortening the current standard therapy (7, 20, 30).

We have presented intracellular killing kinetics for 6 different fluoroquinolone drugs assessed using two methods. The first method is useful for rapid ranking of the potency of the various drugs resulting in concentration-effect relationships (Table S1). This allows for the identification of the best candidates for further analysis. The results demonstrated that 4 out of the 6 fluoroquinolones have similar potencies (MXF, LVX, CIP, SPX). Despite RIF, our control compound, being superior overall, MXF displayed a similar maximal kill rate in both the live fluorimetry and the fixed Operetta assay. Yet, patients treated with a 4-month regimen containing MXF showed higher rates of disease relapse despite achieving faster culture conversion in comparison to standard treatments (11). MXF however, has superior PK properties compared to a standard regimen of RIF (which is currently dosed sub-optimally), especially in its accumulation in the lung and ELF. The high accumulation levels compensate for the lower potency when compared to RIF and leads to better overall effect in Monte Carlo simulations, predicting a median culture conversion time of 31 days compared to 56 days for standard treatment.

Our intracellular data was in agreement with data from a murine macrophage study, showing that NOX and OXF are significantly less potent than MXF (32). Whilst SPX displayed the lowest EC_{50}, cytotoxicity was observed as reported in the literature (33) therefore it was eliminated from further investigation. MXF, CIP and LVX showed similar potency and maximal kill rates. CIP displayed a similar EC_{50} to MXF in our study but at 500 mg it has 10-fold lower exposure in the ELF when compared to MXF

at 400 mg (25). Therefore, only MXF and LVX were considered further in our analyses. A 1000 mg dose of LVX has a comparable ELF AUC value (221.7 mg.h/L) compared to a standard dose of MXF of 400 mg/day (173.1 mg.h/L, Table S4) and that at this higher dose, the clinical efficacy of LVX, in terms of culture conversion rates, is predicted by the *PDi*-based modelling to be comparable to MXF (Fig. 5). This observation is consistent with a recent clinical study comparing MXF (400 mg) to high dose (750 mg) LVX, demonstrating that both regimens results in a similar clinical outcome (34, 35). These data support that, in the absence of any safety concerns, LVX should be further trialed at higher doses.

Similar to the work described previously (22), we show that it is the intracellular kill rate of MXF that limits the reduction of CFU burden, even when the intracellular population represents just 5% of the overall population (with in our model 95% represented by extracellular *Mtb*). Supplementary figure 4 displays the biexponential nature of CFU reduction which, in our simulation, is a direct result of having two separate populations (extracellular and intracellular) (Fig. S4).

That our *PDi*-based modelling approach (using short-term measurements of intracellular *Mtb* killing) is able to predict long-term clinical responses, is perhaps not surprising when it is considered that the majority of patients (*ca*. 80 %) culture convert within *ca*. 8 weeks of treatment (36). We have previously shown that clinical biphasic treatment responses can be explained by an initial reduction in extracellular *Mtb* followed by a second slower phase of bacillary clearance that largely corresponds to the killing dynamics of intracellular (macrophage) *Mtb* (22, 37). The duration of this second slower bacillary clearance rate is typically 5-6 weeks. Therefore, the *PDi*-based modelling approach should be viewed as a predictive tool to determine the clinical response over this shorter time-frame, which is nonetheless a critical clinical feature to assess drug efficacy. Clearly, the *PDi*-based modelling approach does not take into account the response to treatment of slow growing/dormant bacilli, which are thought to be relevant to TB treatment outcome (38). However, given the strong agreement in the *PDi*-based modelling to observed clinical bacillary clearance responses, it is our view that these important PD and PK considerations are more relevant in terms of predicting microbiological treatment outcomes and potentially treatment relapse rates. As described, this study proposes that a useful proxy to

296 estimating disease relapse is the treatment duration *post* culture conversion, and
297 therefore knowledge of bacillary clearance rates for drugs and drug combinations can
298 be used to inform treatment outcome and relapse rates.
299 **Should MXF be introduced to the standard treatment?**
300
301 Incorporating MXF into treatment regimens results in faster clearance rates of bacilli
302 compared to standard treatment in 8 different clinical studies (39). As
303 aforementioned, Gillespie *et al*. 2014 showed that a 4-month MXF based treatment
304 results in a higher relapse rate (11, 21). Superior culture conversion results indicate
305 that relapse rates should be lower in the MXF arm. *PDi* simulations can accurately
306 predict the percentage of patients reaching culture-negative status when compared to
307 observed clinical findings (Table S2). Additionally, sensitivity analysis (Table S3)
308 indicates that MXF in these regimens is the main driver of activity in combination
309 treatments and its effect significantly supersedes that of RIF, thus explaining the
310 accelerated clearance of bacilli when MXF is introduced to the drug regimen.
311
312 However, the culture conversion rates in clinical findings did not predict the high
313 relapse rate in the MXF arm that was reported in Gillespie *et al*. 2014. One
314 explanation of this disparity between bacilli clearance rates and disease relapse could
315 be related to length of time treatment is received after achieving negative culture
316 conversion. This will vary between individual patients. We hypothesise that each
317 patient requires treatment exceeding 80-days following culture conversion. For
318 example, according to our *PDi* predictions, in the 4-month MXF arm 12% - 17% of
319 patients will be at risk of relapse as they will culture convert late and receive
320 treatment for less than 80-days after culture converting (Fig. 6). In contrast, only 7%
321 will be at risk of relapse in the standard 6-month arm. The remaining 93% will
322 remain on treatment for more than 80-days after culture conversion. We have
323 suggested an 80-day duration post culture conversion, because this is the duration that
324 predicts 15% relapse rate which agrees with relapse rates observed in the Gillespie *et*
325 *al.* 2014 clinical trial with MXF containing regimens. This correlation between
326 delayed culture conversion and relapse rate has previously been suggested (40)
327 although this seems to be with limitations as many patients with delayed culture
328 conversion might still have favourable outcomes. Based on our data and simulations,
329 introducing MXF into the standard regimen could lead to a reduced treatment period

e.g. from 6 to 5-months. These findings further support the notion of individualised therapy, where patients with late culture conversion could receive treatment for longer durations than those with early culture conversion (41).

Conclusions

Our preclinical model may offer an insight into the performance of compounds with the overall aim of reducing the TB treatment period down from 6-months. By adding MXF into the regimen, we predicted the treatment outcome and could offer recommendations for its use in the clinic. Although results from previous clinical trials were disappointing when substituting MXF into the standard regimen, it is a well-tolerated compound with high anti-mycobacterial and favourable ELF properties. Based on our modelling, MXF and LVX have the potential to shorten the treatment period and our data aligns with independent clinical results. The individual timeframe for which a patient converts to a culture-negative status is particularly important when determining treatment duration, and a more individual based therapy would be highly beneficial in reducing treatment duration and potentially in reducing relapse rates.

Materials and Methods

Chemical Compounds

The fluoroquinolones moxifloxacin (MXF), levofloxacin (LVX), norofloxacin (NOX), ofloxacin (OFX), sparfloxacin (SPX), and ciprofloxacin (CIP) were purchased from Sigma, UK. All compounds were made up in DMSO (Sigma).

Mycobacterial Strain, Growth and Macrophage Growth

Mtb H37Rv expressing the far-red reporter mCherry, was used in this study (H37Rv-mCherry) (22). Aliquots of H37Rv-mCherry was pre-cultured aerobically at 37°C in Middlebrook 7H9 broth (Difco) supplemented with 0.05% (v/v) Tween 80 (Sigma),

0.2% (v/v) glycerol, 10% oleic acid-albumin-dextrose-catalase (OADC) (7H9) and 50 mg/L hygromycin (Sigma) with magnetic stirrers. THP-1 cells were routinely cultured in RPMI 1640 supplemented with L-Glutamine, $NaHCO_3$ (Gibco) and 10% heat-inactivated fetal bovine serum (HI-FBS; Gibco), at 37˚C, 5% CO_2.

Macrophage Infection Assay

THP-1 cells were differentiated in PerkinElmer® CellCarrier-96 plates, seeded at 5 × 10^5 cells per well and differentiated for 72 h in supplemented RPMI 1640 and 100 ng/mL phorbol 12-myristate 13-acetate (PMA; Sigma) at 37˚C, 5% CO_2. Differentiated THP-1 cells were infected with H37Rv-mCherry in suspension at a multiplicity of infection (MOI) of 1:5 in FluoroBrite™ DMEM supplemented with 10% HI-FBS and L-Glutamine for 24 h at 37°C. For optimal macrophage environment, each 96 well plate was covered with a Breath-EASIER™ sealing membrane (Sigma) to allow gaseous exchange but maintaining containment level 3 safety regulations. This has been refined from our previous work, improving the THP-1 cell growth conditions. After 24 h the cells were washed, the drugs at required concentrations were added in FluoroBrite™ DMEM$^+$ to a total volume of 200 µL. Infected cells were incubated for up to 144 h.

Extracellular-grown (planktonic) *Mtb* kill kinetics were obtained by incubating *Mtb* H37Rv in the presence of test drug followed by plating to obtain colony forming units (CFUs). *Mtb* was cultured at 37°C in Middlebrook 7H9 broth (Difco) supplemented with 0.05% (v/v) Tween 80 (Sigma), 0.2% (v/v) glycerol, 10% oleic acid-albumin-dextrose-catalase (OADC) (7H9) and 50 mg/L hygromycin (Sigma) with magnetic stirrers, to the mid-log growth phase before two-fold dilutions of test drug ranging from 15360 to 30 ng/mL were added. A sample of culture was plated at 0 h before drug was added to obtain the initial bacterial count. After the addition of drug, 2 mL aliquots of bacterial culture with magnetic stirrers were incubated at 37°C in complete media. At defined time intervals of 24, 48, 72, 96, and 168 h, aliquots were pelleted to remove drug. These were serially diluted in PBS, plated on Middlebrook 7H11 agar and incubated at 37°C in 5% CO_2 for 28 days. The Miles Misra method was used to determine CFUs (42).

Fluorometer Drug Screening, High-content Image Acquisition and Data Analysis

Data were generated from multiple independent experiments ($n \geq 3$) all performed at least in triplicate and data were produced via two methods. First, each plate was screened every 24 h for fluorescence using a Varioskan (LUX™ multimode reader, Thermo Scientific™) at an excitation (ex) of 578 nm and emission (em) of 610 nm thus producing 'live' fluorometer readouts. Additionally, plates were fixed with 5% paraformaldehyde (PFA) (Sigma) for 2 h for imaging using an Operetta (PerkinElmer®) with a 60x High NA objective as described previously (22).

The *Z′*-factor for the Varioskan assay was calculated according to equation 1 as reported in Zhang *et al*. 1999 (43) and calculated to be 0.57 for the data set.

Unlike the Operetta-based high content imaging screen, maximum kill rates cannot be calculated from the fluorometer. Upon bacilli death, the measured linear response of *Mtb* to a compound eventually plateaus limiting the dynamic range of the assay.

Data Analysis and Modelling

Fluoroquinolone activity was ranked using the Varioskan fluorimeter readout. An algorithm was used for drug combinations where the overall kill rate at any given time is equal to the kill rate of the drug with the highest kill rate at that given time point (this kill rate is dependent on the changing of a drug's concentration and its constant PD parameters [EC_{50} and E_{max}]). Hence, the model assumes that there are no positive or negative PD interactions between the drugs (31). Bacterial growth and death rates at differing drug concentrations were measured using Pmetrics GraphPad Prism® per the following equation:

$$Mtb\ count = initial\ Mtb\ count \cdot (1 - exp(-K * x)) \ldots\ldots \text{ eq.2}$$

Where K represents the growth rate per hour and would be a negative value if the bacterial count is decreasing over time. Each drug concentration generated an independent K value. This value was normalised to bacterial growth per experiment to avoid inter-experimental bias and thus the growth rate was divided by the K value to normalise the kill rate. Kill rates at different concentrations are then fitted to a 3-parameter pharmacological model per the following equation using Graphpad Prism®:

$$E = \frac{E_{max} \cdot C}{EC_{50} + C} + E_{min} \quad \ldots\ldots \text{ eq.3}$$

Where E is the kill rate at any given concentration, Emax is the maximal kill rate of each drug, C is the drug concentration in mg/L and EC_{50} is concentration required to achieve half the maximal kill rate.

Extracellular-grown *Mtb* kill rates and EC_{50} values for RIF, INH and EMB, were derived from our previous study (22), while MXF extracellular EC_{50} (356 ng/mL) and kill rate ($0.23h^{-1}$) were derived in this study (Fig. S5). LVX extracellular E_{max} and EC_{50} were assumed to be similar to MXF for the purposes of this work.

Modelling parameters

Parameters for RIF, INH, PZA and EMB were derived from our previous work (22), whereas parameters for fluoroquinolone drugs were derived from experiments described herein. Supplementary Table 5 summarises the parameters used for the simulation with the corresponding references.

We observed a very strong correlation between the growth rate and the corresponding kill rate in all experiments for all drugs screened. RIF and MXF exhibited similar maximal kill rates that always varied between 1.6-2-fold higher than the growth rate, regardless if the latter was fast or slow. The consistency in the ratio between the growth and kill rates allows the ability to correct all data to a fixed growth rate, in all simulations, to reduce output noise whilst not compromising the final outcomes. Reported intracellular *Mtb* growth rates (also known as doubling times, DT),

including those reported by us, range from DT 21 h to DT 48 h, (22, 44, 45) whilst *in vivo* rodent TB models report an intracellular DT for *Mtb* close to 25 h (46). The reason for the reported variation is not fully understood, but could be partially explained by macrophage modulation of M0/M1/M2 polarisation (37). For the described *PDi*-based modelling approach, we chose a DT of 21 h for consistency with previous studies and to avoid bias in cross-study comparisons in the future.

Monte Carlo Simulations

Monte Carlo simulations for PK/PD predictions were performed using Pmetrics® with PK parameters derived from the literature. PK values for MXF were chosen from studies where MXF was administered with RIF, due to the known PK interaction between the two drugs (23, 24). PK for other standard drugs were used as previously described (22).

The models utilised for Monte Carlo simulations herein were previously described in detail in (22, 31). Briefly, the CFU reduction in each simulated patient was driven by exposure to drug and kill rate of each drug according to an Emax model (Eq. 3). Extracellular and intracellular bacilli respond differently to drug treatment and both reservoirs were simultaneously simulated for each patient, resulting in a biexponential decrease in total CFU burden over time (Fig. S3). Overall drug kill rate (of all drugs in combination) is equal to the rate of the fastest acting drug at the same time. This is determined by the epithelial lining fluid (ELF) drug exposure and its intrinsic rate of kill (as defined *in vitro*) at any given time point for each drug.

Initial clinical colony-forming unit (CFU) count in each of the 1000 simulated patients' lungs was assumed to be 10^7 CFU/mL (22). All PK profiles for analysis were assumed to follow a 1-compartment model. Pulmonary levels of drug which were assumed to be the driver for activity (where C in equation 2 represents drug concentration in the ELF); ELF levels were estimated by using ELF:Serum ratio reported in the literature as previously described for RIF, ETB, INH and PZA and an ELF ratio of 5.2 was estimated for MXF (47). The CFU change was recorded over time at fixed intervals of 1 week over a simulated run time of 4-months

(MXF+RIF+INH+PZA) containing regimens) to 6-months (standard regimen). It was assumed that a 10 CFU/mL or lower outcome at any given time would indicate culture conversion to be negative, as previously described (22). The number of patients converting to culture negative status in the simulation every week was then recorded for further survival analysis. Supplementary Table 5 summarises the parameters used for the simulation with the corresponding references.

Odds ratios were calculated using IBM® SPSS® Statistics Version 24 (property of IBM Corp). Data generated form Monte Carlo simulation from different scenarios were compared head to head and the odds ratio with 95CI was estimated accordingly.

Sensitivity analysis was performed to assess the most influential parameters upon the bacillary clearance within the simulation (Table S3). The analyses were performed using the FME package (A Flexible Modelling Environment for Inverse Modelling, Sensitivity, Identifiability and Monte Carlo Analysis) with R version 3.4.2 (48). Influence of each parameter was expressed in terms of L1-norm and L2-norm measures which rank parameters by their effect upon the simulation. The higher the L1-norm or L2-norm for a given parameter, the higher the sensitivity (49). Sensitivity analysis (Table S3) shows that MXF would be the main driver of activity in a combination of drugs. This is further corroborated by observing the changing kill rate over time for each of the partner drugs which shows that MXF dominates as the fastest killer throughout the treatment duration, followed by RIF while INH and PZA play a negligible role in the overall clearance of bacilli (Fig. S5).

Methodological assumptions and limitations

Whilst fluorimetric-based measurements of intracellular *Mtb* can effectively measure bacillary growth, this approach has a limited dynamic range when assessing bacillary sterilisation over time when measurements fall below the minimum limit of fluorescence detection. To overcome this issue, high-content (Operetta) imaging was used to more accurately measure time-dependent bacillary sterilisation for specific drugs. With regards to intracellular *Mtb* growth, during the course of this and our other studies, as well as in studies by other laboratories, we noted a variation in

intracellular *Mtb* DT, as aforementioned in the 'Modelling Parameters' section. To normalise for this in our mathematical modelling, we selected a DT of 21 h throughout. Furthermore, for the purpose of the mathematical modelling/simulations to predict clinical outcome, in the absence of evidence to the contrary, we also made a number of assumptions, including; (i) it was assumed that there is no pharmacological interaction [synergy/additivity/antagonism] between the modelled drugs, therefore the clinically observed *Mtb* sterilisation rate was equivalent to the sterilisation rate of the drug with the fastest sterilisation rate. It was also hypothesised that (ii) PD interactions of drugs against intracellular (macrophage) *Mtb* measured in *in vitro* culture were similar to those in the ELF.

It should be noted that whilst time-dependent intracellular *Mtb* sterilisation rates and *PDi* -PK modelling have been used in this study to predict the clinical activity of fluoroquinolones against TB, this approach generates dynamic parameters (e.g. EC_{50} and E_{max}) that are not suitable for comparison with traditional static microbiological parameters such as MIC.

Acknowledgments

General: Dr. Derek Sloan from the University of St Andrews is thanked for reading of the manuscript and useful discussions.

Funding: This work was supported in part by the Medical Research Council (G1002586, MR/N028376/1 and MC_PC_14111, GAB and SAW), the Wellcome Trust (105620/Z/14/Z, GAB and SAW), and by the PreDiCT-TB consortium (http://www.predict-tb.eu) funded from the Innovative Medicines Initiative Joint Undertaking (http://www.imi.europa.eu [grant agreement number No. 115337 to GAB and SAW]), resources of which are composed of financial contribution from the European Union's Seventh Framework Programme [FP7/2007–2013] and EFPIA companies' in kind contribution.

Author contributions: G.A.B. conceived the study, designed and interpreted the experiments. S.A.W. study design and data interpretation. S.D. study design, data interpretation, data analyses and experimental. G.A. study design, data interpretation and PKPD analyses. A.A., E.M. and C.M.R. assisted in *Mycobacterium tuberculosis* culture and time-dependent killing assays. All authors contributed to writing of the manuscript.

Competing interests: The authors have no competing interests.

References

1. WHO. 2017. TUBERCULOSIS GLOBAL REPORT.
2. Ji B, Lounis N, Maslo C, Truffot-Pernot C, Bonnafous P, Grosset J. 1998. In vitro and in vivo activities of moxifloxacin and clinafloxacin against Mycobacterium tuberculosis. Antimicrob Agents Chemother 42:2066–2069.
3. Miyazaki E, Miyazaki M, Chen JM, Chaisson RE, Bishai WR. 1999. Moxifloxacin (BAY12-8039), a new 8-methoxyquinolone, is active in a mouse model of tuberculosis. Antimicrob Agents Chemother 43:85–89.
4. Rodriguez JC, Ruiz M, Lopez M, Royo G. 2002. In vitro activity of moxifloxacin, levofloxacin, gatifloxacin and linezolid against Mycobacterium tuberculosis. Int J Antimicrob Agents 20:464–467.
5. Fattorini L, Tan D, Iona E, Mattei M, Giannoni F, Brunori L, Recchia S, Orefici G. 2003. Activities of moxifloxacin alone and in combination with other antimicrobial agents against multidrug-resistant Mycobacterium tuberculosis infection in BALB/c mice. Antimicrob Agents Chemother 47:360–362.
6. Nuermberger EL, Yoshimatsu T, Tyagi S, O'Brien RJ, Vernon AN, Chaisson RE, Bishai WR, Grosset JH. 2004. Moxifloxacin-containing regimen greatly reduces time to culture conversion in murine tuberculosis. Am J Respir Crit Care Med 169:421–426.
7. Gillespie SH. 2016. The role of moxifloxacin in tuberculosis therapy. Eur Respir Rev 25:19–28.
8. Gninafon M, Lo MB, Mthiyane T, Sc M, Kassa F, Diaye AN, Rustomjee R, Jong BC De, Ph D, Horton J, Perronne C, Sismanidis C, Ph D, Lapujade O, Sc B, Merle CS, Fielding K, Sow OB, Gninafon M, Lo MB, Mthiyane T, Odhiambo J, Amukoye E, Bah B, Kassa F, N'Diaye A, Rustomjee R, de Jong BC, Horton J, Perronne C, Sismanidis C, Lapujade O, Olliaro PL, Lienhardt C. 2014. A Four-Month Gatifloxacin-Containing Regimen for Treating Tuberculosis. N Engl J Med 371:1588–1598.
9. Rustomjee R, Lienhardt C, Kanyok T, Davies GR, Levin J, Mthiyane T, Reddy C, Sturm AW, Sirgel FA, Allen J, Coleman DJ, Fourie B, Mitchison DA,

Gatifloxacin for TB study team. 2008. A Phase II study of the sterilising activities of ofloxacin, gatifloxacin and moxifloxacin in pulmonary tuberculosis. Int J Tuberc Lung Dis 12:128–138.
10. Conde MB, Efron A, Loredo C, De Souza GR, Graca NP, Cezar MC, Ram M, Chaudhary MA, Bishai WR, Kritski AL, Chaisson RE. 2009. Moxifloxacin versus ethambutol in the initial treatment of tuberculosis: a double-blind, randomised, controlled phase II trial. Lancet 373:1183–1189.
11. Gillespie SH, Crook AM, McHugh TD, Mendel CM, Meredith SK, Murray SR, Pappas F, Phillips PPJ, Nunn AJ. 2014. Four-Month Moxifloxacin-Based Regimens for Drug-Sensitive Tuberculosis. N Engl J Med 371:1577–1587.
12. Burman WJ, Goldberg S, Johnson JL, Muzanye G, Engle M, Mosher AW, Choudhri S, Daley CL, Munsiff SS, Zhao Z, Vernon A, Chaisson RE. 2006. Moxifloxacin versus ethambutol in the first 2 months of treatment for pulmonary tuberculosis. Am J Respir Crit Care Med 174:331–338.
13. Xu P, Chen H, Xu J, Wu M, Zhu X, Wang F, Chen S, Xu J. 2017. Moxifloxacin is an effective and safe candidate agent for tuberculosis treatment: a meta-analysis. Int J Infect Dis 60:35–41.
14. Bartelink IH, Zhang N, Keizer RJ, Strydom N, Converse PJ, Dooley KE, Nuermberger EL, Savic RM. 2017. New Paradigm for Translational Modeling to Predict Long-term Tuberculosis Treatment Response. Clin Transl Sci.
15. Lanoix J, Loerger T, Ormond A, Kaya F, Sacchettini J, Dartois V, Nuermberger E. 2015. Selective inactivity of pyrazinamide against tuberculosis in C3HeB/FeJ mice is best explained by neutral pH of caseum. Antimicrob Agents Chemother 16:735–743.
16. Rosenthal IM, Tasneen R, Peloquin CA, Zhang M, Almeida D, Mdluli KE, Karakousis PC, Grosset JH, Nuermberger EL. 2012. Dose-ranging comparison of rifampin and rifapentine in two pathologically distinct murine models of tuberculosis. Antimicrob Agents Chemother 56:4331–4340.
17. de Steenwinkel JE, Aarnoutse RE, de Knegt GJ, ten Kate MT, Teulen M, Verbrugh HA, Boeree MJ, van Soolingen D, Bakker-Woudenberg IA. 2013. Optimization of the rifampin dosage to improve the therapeutic efficacy in tuberculosis treatment using a murine model. Am J Respir Crit Care Med 187:1127–1134.
18. Weiner M, Savic RM, Kenzie WR, Wing D, Peloquin CA, Engle M, Bliven E,

Prihoda TJ, Gelfond JA, Scott NA, Abdel-Rahman SM, Kearns GL, Burman WJ, Sterling TR, Villarino ME, Tuberculosis Trials Consortium PTBPG. 2014. Rifapentine Pharmacokinetics and Tolerability in Children and Adults Treated Once Weekly With Rifapentine and Isoniazid for Latent Tuberculosis Infection. J Pediatr Infect Dis Soc 3:132–145.

19. Rosenthal IM, Zhang M, Almeida D, Grosset JH, Nuermberger EL. 2008. Isoniazid or moxifloxacin in rifapentine-based regimens for experimental tuberculosis? Am J Respir Crit Care Med 178:989–993.

20. Lanoix E, Chaisson R, Nuermberger E. 2016. Shortening tuberculosis treatment with fluoroquinolones: lost in translation? Clin Infect Dis 62:484–90.

21. Jindani A, Harrison TS, Nunn AJ, Phillips PPJ, Churchyard GJ, Charalambous S, Hatherill M, Geldenhuys H, McIlleron HM, Zvada SP, Mungofa S, Shah NA, Zizhou S, Magweta L, Shepherd J, Nyirenda S, van Dijk JH, Clouting HE, Coleman D, Bateson ALE, McHugh TD, Butcher PD, Mitchison DA. 2014. High-Dose Rifapentine with Moxifloxacin for Pulmonary Tuberculosis. N Engl J Med 371:1599–1608.

22. Aljayyoussi G, Jenkins VA, Sharma R, Ardrey A, Donnellan S, Ward SA, Biagini GA. 2017. Pharmacokinetic-Pharmacodynamic modelling of intracellular Mycobacterium tuberculosis growth and kill rates is predictive of clinical treatment duration. Sci Rep 7:502.

23. Ramachandran G, Hemanth Kumar AK, Srinivasan R, Geetharani A, Sugirda P, Nandhakumar B, Nandini R, Tharani CB. 2012. Effect of rifampicin & isoniazid on the steady state pharmacokinetics of moxifloxacin. Indian J Med Res 136:979–984.

24. Nijland HMJ, Ruslami R, Suroto AJ, Burger DM, Alisjahbana B, van Crevel R, Aarnoutse RE. 2007. Rifampicin Reduces Plasma Concentrations of Moxifloxacin in Patients with Tuberculosis. Clin Infect Dis 45:1001–1007.

25. Rodvold KA, George JM, Yoo L. 2011. Penetration of anti-infective agents into pulmonary epithelial lining fluid: focus on antibacterial agents. Clin Pharmacokinet 50:637–664.

26. Kiem S, Schentag JJ. 2008. Interpretation of antibiotic concentration ratios measured in epithelial lining fluid. Antimicrob Agents Chemother 52:24–36.

27. Barletta F, Vandelannoote K, Collantes J, Evans CA, Arévalo J, Rigouts L. 2014. Standardization of a TaqMan-based real-time PCR for the detection of

Mycobacterium tuberculosis-complex in human sputum. Am J Trop Med Hyg 91:709–714.

28. Sloan DJ, Mwandumba HC, Garton NJ, Khoo SH, Butterworth AE, Allain TJ, Heyderman RS, Corbett EL, Barer MR, Davies GR. 2015. Pharmacodynamic modeling of bacillary elimination rates and detection of bacterial lipid bodies in sputum to predict and understand outcomes in treatment of pulmonary tuberculosis. Clin Infect Dis 61:1–8.

29. Palaci M, Dietze R, Hadad DJ, Ribeiro FKC, Peres RL, Vinhas SA, Maciel ELN, Dettoni VDV, Horter L, Boom WH, Johnson JL, Eisenach KD. 2007. Cavitary disease and quantitative sputum bacillary load in cases of pulmonary tuberculosis. J Clin Microbiol 45:4064–4066.

30. Thee S, Garcia-Prats AJ, Donald PR, Hesseling AC, Schaaf HS. 2016. Fluoroquinolones for the treatment of tuberculosis in children. Tuberculosis 95:229–245.

31. Aljayyoussi G, Donnellan S, Ward SA, Biagini GA. 2019. Intracellular PD Modelling (PDi) for the Prediction of Clinical Activity of Increased Rifampicin Dosing. Pharmaceutics 11:6–8.

32. Shandil RK, Jayaram R, Kaur P, Gaonkar S, Suresh BL, Mahesh BN, Jayashree R, Nandi V, Bharath S, Balasubramanian V. 2007. Moxifloxacin, ofloxacin, sparfloxacin, and ciprofloxacin against Mycobacterium tuberculosis: Evaluation of in vitro and pharmacodynamic indices that best predict in vivo efficacy. Antimicrob Agents Chemother 51:576–582.

33. Zhanel GG, Walkty A, Vercaigne L, Karlowsky JA, Embil J, Gin AS, Hoban DJ. 1999. The new fluoroquinolones: A critical review. Can J Infect Dis 10:207–238.

34. Koh WJ, Lee SH, Kang YA, Lee CH, Choi JC, Lee JH, Jang SH, Yoo KH, Jung KH, Kim KU, Choi SB, Ryu YJ, Kim KC, Um S, Kwon YS, Kim YH, Choi W Il, Jeon K, Hwang Y Il, Kim SJ, Lee YS, Heo EY, Lee J, WoonKi Y, Shim TS, Yim JJ. 2013. Comparison of levofloxacin versus moxifloxacin for multidrug-resistant tuberculosis. Am J Respir Crit Care Med 188:858–864.

35. Johnson JL, Hadad DJ, Boom WH, Daley CL, Peloquin CA, Eisenach KD, Jankus DD, Debanne SM, Charlebois ED, Maciel E, Palaci M, Dietze R. 2006. Early and extended early bactericidal activity of levofloxacin, gatifloxacin and moxifloxacin in pulmonary tuberculosis. Int J Tuberc Lung Dis 10:605–612.

734 36. Sloan DJ, Davies GR, Khoo SH. 2001. Recent advances in tuberculosis: New
735 drugs and treatment regimens. Antimicrob Agents Chemoterapy 9:1943–1946.
736 37. Huang Z, Luo Q, Guo Y, Chen J, Xiong G, Peng Y, Ye J, Li J. 2015.
737 Mycobacterium tuberculosis-induced polarization of human macrophage
738 orchestrates the formation and development of tuberculous granulomas in vitro.
739 PLoS One 10.
740 38. Fattorini L, Piccaro G, Mustazzolu A, Giannoni F. 2013. Targeting dormant
741 bacilli to fight tuberculosis. Mediterr J Hematol Infect Dis 5:e2013072.
742 39. Xu P, Chen H, Xu J, Wu M, Zhu X, Wang F, Chen S, Xu J. 2017.
743 Moxifloxacin is an effective and safe candidate agent for tuberculosis
744 treatment: a meta-analysis. Int J Infect Dis 60:35–41.
745 40. Phillips PP, Mendel CM, Burger DA, Crook AM, Nunn AJ, Dawson R, Diacon
746 AH, Gillespie SH. 2016. Limited role of culture conversion for decision-
747 making in individual patient care and for advancing novel regimens to
748 confirmatory clinical trials. BMC Med 14:19.
749 41. Imperial MZ, Nahid P, Phillips PPJ, Davies GR, Fielding K, Hanna D,
750 Hermann D, Wallis RS, Johnson JL, Lienhardt C, Savic RM. 2018. A patient-
751 level pooled analysis of treatment-shortening regimens for drug-susceptible
752 pulmonary tuberculosis. Nat Med 24:1.
753 42. Miles AAA, Misra SS, Irwin JO. 1938. The Estimation of the Bactericidal
754 Power of The Blood. J Hyg (Lond) 38:732–749.
755 43. Zhang J, Chung T, Oldenburg K. 1999. A Simple Statistical Parameter for Use
756 in Evaluation and Validation of High Throughput Screening Assays. J Biomol
757 Screen 4:67–73.
758 44. Gill WP, Harik NS, Whiddon MR, Liao RP, Mittler JE, Sherman DR. 2009. A
759 replication clock for Mycobacterium tuberculosis. NIH Public Access 15:211–
760 214.
761 45. Hirota K, Hasegawa T, Nakajima T, Inagawa H, Kohchi C, Soma GI, Makino
762 K, Terada H. 2010. Delivery of rifampicin-PLGA microspheres into alveolar
763 macrophages is promising for treatment of tuberculosis. J Control Release
764 142:339–346.
765 46. Manca C, Tsenova L, Barry 3rd CE, Bergtold A, Freeman S, Haslett PA,
766 Musser JM, Freedman VH, Kaplan G. 1999. Mycobacterium tuberculosis
767 CDC1551 induces a more vigorous host response in vivo and in vitro, but is not

more virulent than other clinical isolates. J Immunol 162:6740–6746.

47. Soman A, Honeybourne D, Andrews J, Jevons G, Wise R. 1999. Concentrations of moxifloxacin in serum and pulmonary compartments following a single 400 mg oral dose in patients undergoing fibre-optic bronchoscopy. J Antimicrob Chemother 44:835–838.

48. Team RC. 2015. A Language and Environment for Statistical Computing.

49. Joliffe I. 2004. Principal Component Analysis (2nd ed.). Springer, New York.

802 **Figures and Tables**

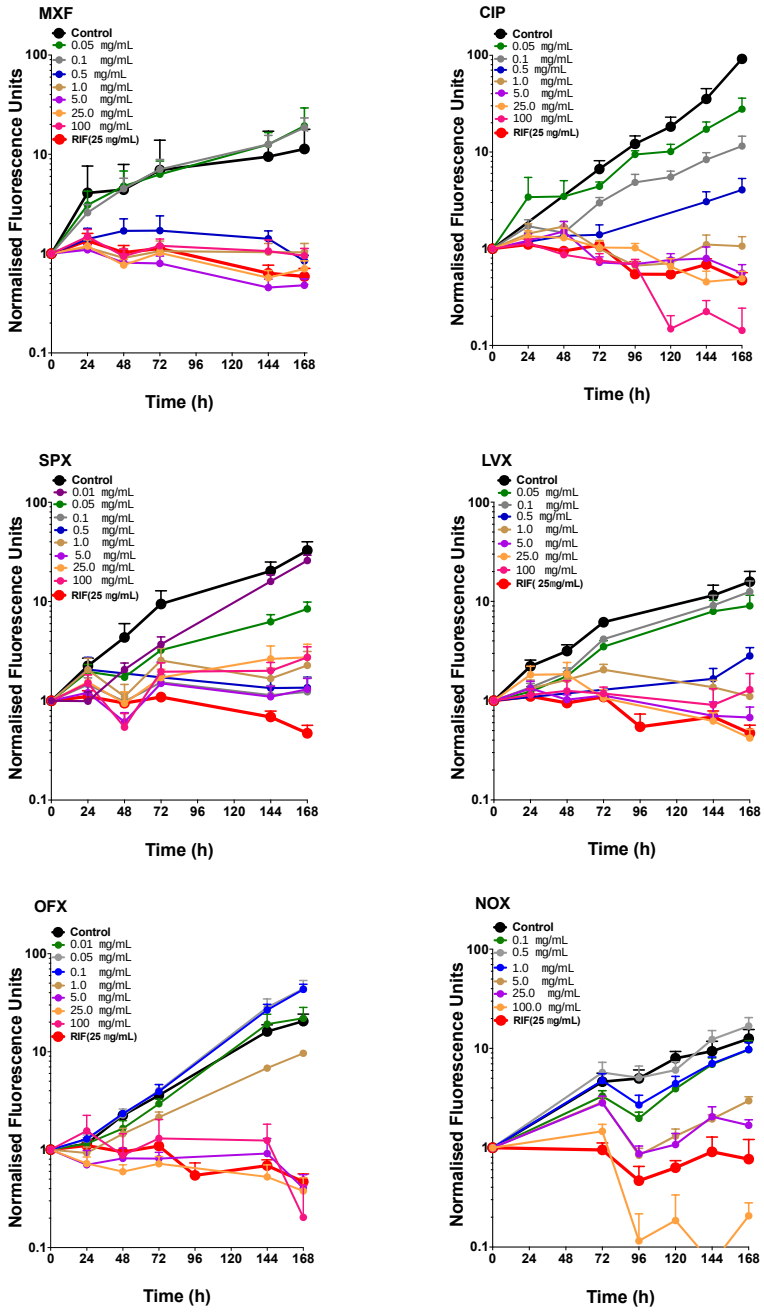

803

804 ***Fig. 1. Intracellular (macrophage) Mtb time-dependent kill profiles of fluoroquinolones.*** *Panels*

805 *display time-kill profiles of (a) MXF, (b) CIP, (c) SPX, (d) LVX, (e) OFX, and (f) NOX. Mtb control*

806 *(no drug) in black and RIF at 25 mg/L in red. Data is mean ± S.D derived from multiple independent*

807 *experiments (n ≥ 3) performed at least in triplicate.*

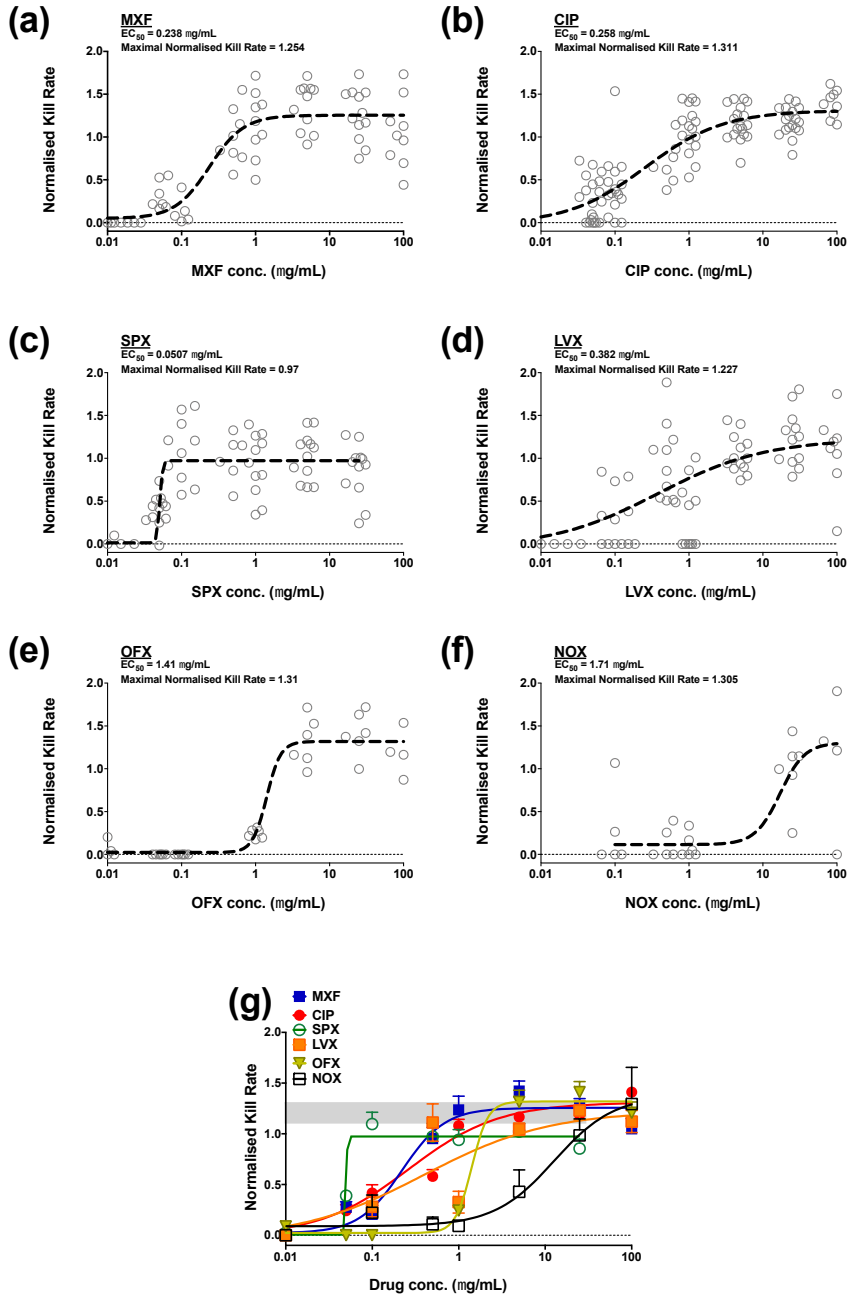

Fig. 2. Concentration-intracellular Mtb kill rate relationship for selected fluoroquinolones

Open black circles represent individual kill rates at each concentration for drugs and the dashed black line displays the 3-parameter pharmacological fit for each drug (a) MXF, (b) CIP, (c) SPX, (d) LVX, (e) OFX, (f) NOX. (g) Represents a comparison of the profiles of all drugs - grey area represents the kill rate of RIF at 25 mg/L. n=6 in 3 independent experimental replicates for each drug.

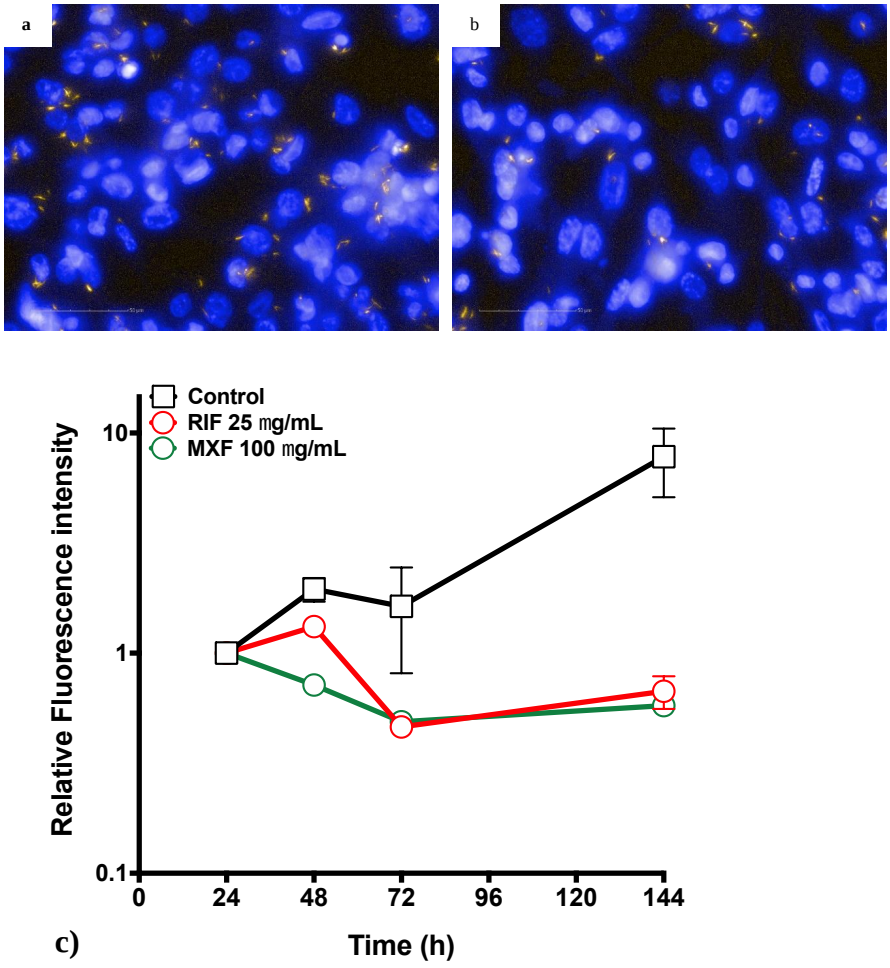

Fig. *3.* ***High-content fluorescent images as acquired from the Operetta (PerkinElmer)***

Fixed macrophages infected with Mtb H37Rv expressing the far-red reporter mCherry after 72 h with (a) no drug treatment or (b) with 100 mg/L MXF. H37Rv-mCherry (orange), macrophage nuclei stained with Hoechst (blue), scale bar 50 µm, (c) represents activity of MXF against intracellular Mtb (data acquired from the Operetta via Harmony, PerkinElmer) with the red solid line displaying the maximal kill rate obtained by RIF at 25 mg/L.

833

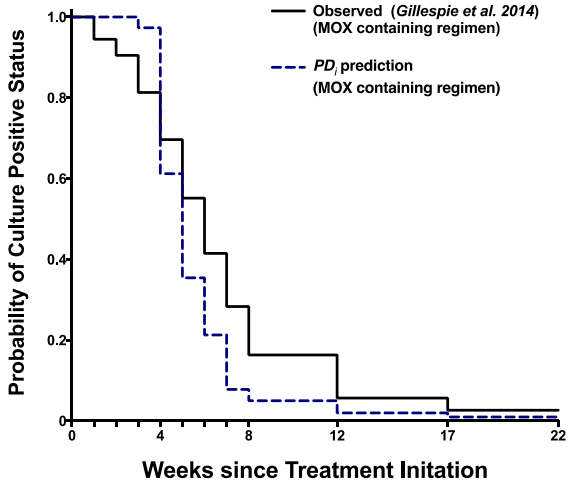

834

835 a)

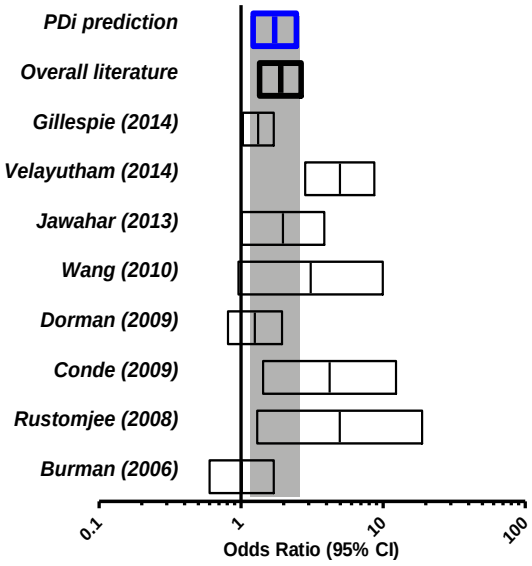

836

837 b)

838

839 ***Fig. 4. Culture conversion rates and forest plot of odds ratios***

840 *(a) Observed culture conversion rates from patients treated with MXF+RIF+EMB+PZA for 4-months*

841 *in a clinical study by Gillespie et al. 2014 (solid black line) compared to our PDi prediction for the*

842 *same dosing regimen over the same duration (dashed blue line). (b) Forest plot showing odds ratios*

843 *from 8 clinical studies (39) compared to odds ratio calculated using our PDi based Monte Carlo*

844 *simulations. Grey area represents range of PDi prediction.*

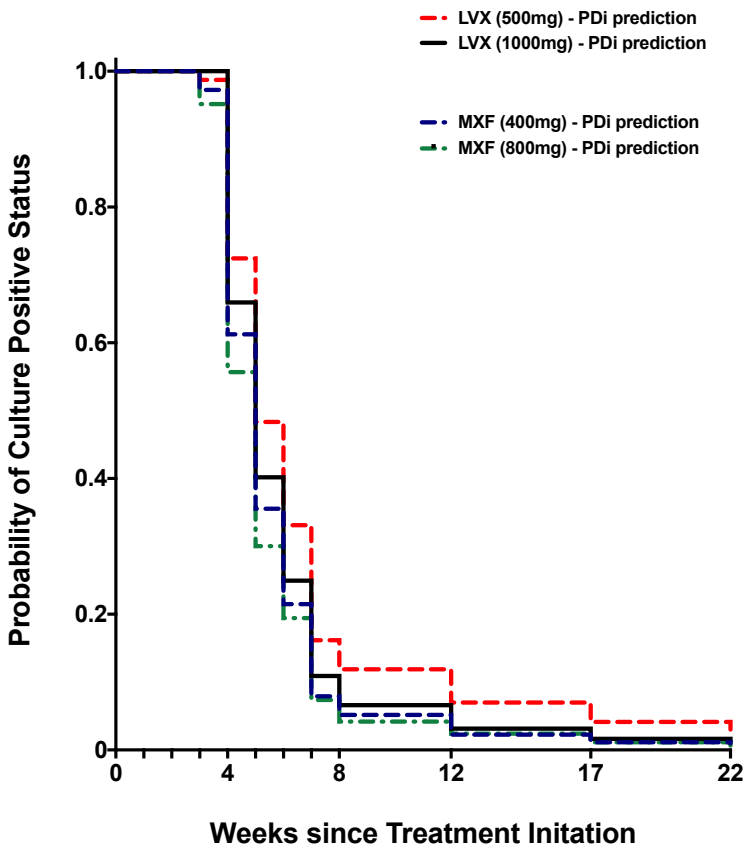

Fig. 5. PDi predictions

PDi prediction of culture conversion rates for MXF (400 mg daily, 4-months, dashed blue line) Vs. LVX (1000 mg daily, 4-months, solid black line), LVX (500 mg daily, 4-months, dashed red line) and MXF (800 mg daily, dashed green line).

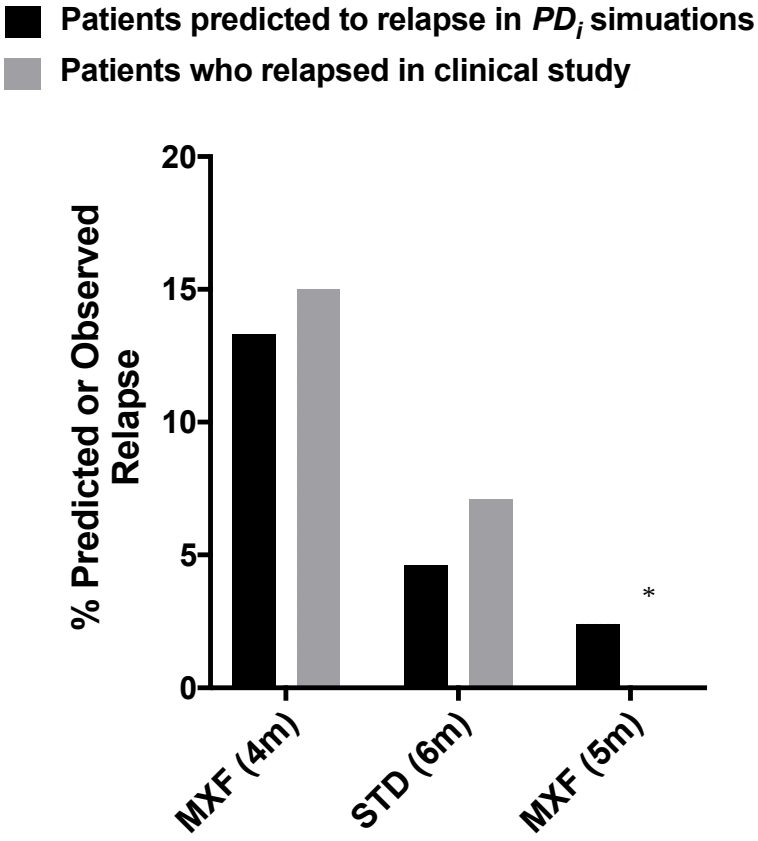

Fig. 6. Predicted or observed relapse rates

*The % of patients that are predicted to relapse (based on late culture conversion status) (black bars) compared to observed relapse rates as observed in Gillespie et al. 2014 (grey bars). The observed relapse rates are based on both MXF arms in the clinical study. * 5 month MXF data not available.*